

**Molecular Dynamics and Monte Carlo simulations in the microcanonical ensemble:
Quantitative comparison and reweighting techniques**

Philipp Schierz, Johannes Zierenberg, and Wolfhard Janke

Citation: *The Journal of Chemical Physics* **143**, 134114 (2015); doi: 10.1063/1.4931484

View online: <http://dx.doi.org/10.1063/1.4931484>

View Table of Contents: <http://scitation.aip.org/content/aip/journal/jcp/143/13?ver=pdfcov>

Published by the [AIP Publishing](#)

Articles you may be interested in

[Extended Lagrangian Born-Oppenheimer molecular dynamics simulations of the shock-induced chemistry of phenylacetylene](#)

J. Chem. Phys. **142**, 064512 (2015); 10.1063/1.4907909

[Generalized Metropolis acceptance criterion for hybrid non-equilibrium molecular dynamics—Monte Carlo simulations](#)

J. Chem. Phys. **142**, 024101 (2015); 10.1063/1.4904889

[Liquid-vapor isotopic fractionation factors of diatomic fluids: A direct comparison between molecular simulation and experiment](#)

J. Chem. Phys. **125**, 034510 (2006); 10.1063/1.2215611

[Monte Carlo simulations with first-principles energies](#)

AIP Conf. Proc. **577**, 166 (2001); 10.1063/1.1390186

[Equilibrium thermodynamics of homopolymers and clusters: Molecular dynamics and Monte Carlo simulations of systems with square-well interactions](#)

J. Chem. Phys. **107**, 10691 (1997); 10.1063/1.474186



AIP | APL Photonics

APL Photonics is pleased to announce
Benjamin Eggleton as its Editor-in-Chief



Molecular Dynamics and Monte Carlo simulations in the microcanonical ensemble: Quantitative comparison and reweighting techniques

Philipp Schierz,^{a)} Johannes Zierenberg,^{b)} and Wolfhard Janke^{c)}
Institut für Theoretische Physik, Universität Leipzig, Postfach 100 920, 04009 Leipzig, Germany

(Received 11 June 2015; accepted 8 September 2015; published online 6 October 2015)

Molecular Dynamics (MD) and Monte Carlo (MC) simulations are the most popular simulation techniques for many-particle systems. Although they are often applied to similar systems, it is unclear to which extent one has to expect quantitative agreement of the two simulation techniques. In this work, we present a quantitative comparison of MD and MC simulations in the microcanonical ensemble. For three test examples, we study first- and second-order phase transitions with a focus on liquid-gas like transitions. We present MD analysis techniques to compensate for conservation law effects due to linear and angular momentum conservation. Additionally, we apply the weighted histogram analysis method to microcanonical histograms reweighted from MD simulations. By this means, we are able to estimate the density of states from many microcanonical simulations at various total energies. This further allows us to compute estimates of canonical expectation values. © 2015 AIP Publishing LLC. [<http://dx.doi.org/10.1063/1.4931484>]

I. INTRODUCTION

In the last years, Monte Carlo (MC) simulations were used to study phase transitions in the microcanonical ensemble for various systems.^{1–5} One of the main reasons was that the microcanonical ensemble highlighted some system properties in the phase transition region which could not be observed in the canonical ensemble.⁶ The work of Martin-Mayor⁴ even suggested that one can distribute the computational effort regarding the exponential slowing down at a first-order phase transition to several simulations in the microcanonical ensemble at different total energies.

The microcanonical (NVE) ensemble at fixed particle number N , volume V , and total energy E is motivated by fundamental statistical mechanics. By integrating the classical Newton's equations of motion, Molecular Dynamics (MD) simulations obtain trajectories for which, if ergodic sampling is achievable, the time averages should coincide with the appropriate ensemble averages estimated in MC simulations. The conservation of the total energy is automatically guaranteed in MD simulations with conservative forces up to discretization errors due to the numerical integration and round-off errors. Consequently, the temperature T becomes an observable. This behavior is quite counterintuitive if one is used to the canonical (NVT) ensemble.

The main focus of this paper is on a quantitative comparison of microcanonical MD and microcanonical MC simulations for three exemplary phase transitions. There exist, of course, already studies concerning the comparability of MD and MC simulations,^{7–15} but we encountered special problems

for the liquid-gas like phase transition at fixed density which have, to our knowledge, not been addressed in the literature so far. Because of the small scale of the investigated systems in this work, we like to highlight that what we will call “phase transitions” are always “pseudo-phase transitions” with regard to the small particle numbers.

MD simulations show some particularities in connection with the conservation laws for linear momentum \mathbf{P} and angular momentum \mathbf{J} . Those conservation laws are leading to restrictions of the phase space in comparison with the NVE ensemble which was already described, for example, by Honeycutt and Andersen.⁹ The effects of those conservation laws on observable averages are, of course, only prominent for a small number of degrees of freedom. Today it is common to investigate systems in the so-called “mesoscopic” scale with length scales much larger than the atomistic but below the micrometer scale. This is usually achieved by employing coarse-grained models with a moderate number of degrees of freedom f satisfying $f \gg 1$ but $f \ll \infty$. Recent examples are investigations of single polymer collapse by Seaton *et al.*¹⁶ or Marenz *et al.*¹⁷ Two exemplary systems in this work fall into this mesoscopic scale, whereas the third system is situated at the atomistic scale with only few degrees of freedom.

MD simulations with periodic boundary conditions (PBCs) sample either in the NVEP ensemble (all microcanonical phase space points with a fixed total linear momentum) or NVEPJ ensemble (all microcanonical phase space points with a fixed total linear and angular momentum).^{12,18} While observing a liquid-gas like phase transition, one encounters transits between those two ensembles in MD simulations. For a larger number of degrees of freedom, the difference between the observable averages in the NVE, NVEP, or NVEPJ ensemble shrinks.¹⁹ The standard temperature definition according to the equipartition theorem is via the average kinetic energy,

^{a)}Electronic mail: philipp.schierz@itp.uni-leipzig.de

^{b)}Electronic mail: johannes.zierenberg@itp.uni-leipzig.de

^{c)}Electronic mail: wolfhard.janke@itp.uni-leipzig.de

$$T = \frac{2}{fk_B} \langle E_k \rangle, \quad (1)$$

where f is the number of degrees of freedom in momentum space ($f = 3N$ without constraints), k_B is the Boltzmann constant (here $k_B = 1$), and kinetic energy $E_k = \sum_{i=1}^N \mathbf{p}_i^2 / 2m_i$, with particle momenta \mathbf{p}_i and masses m_i . This definition accounts for the number of degrees of freedom and is therefore one commonly used way to differentiate energy ranges with and without angular momentum conservation, respectively. In this paper, we propose a time-series reweighting from the sampled NVEP/NVEPJ to the NVE ensemble as an additional way to handle the observable averages.

In addition to the measurement of observables, we aimed to estimate the density of states from MD simulations. For that attempt, it was important to measure histograms correctly and to be aware of the correct ensemble weights (see Sec. II). The advantage is that we can estimate averages at total energies in between the simulated ones. A similar procedure was described in Ref. 10 for the solid-liquid phase transition in a Lennard-Jones system. In this case, the knowledge of the NVEPJ ensemble was completely sufficient for the presented phase transition. In this work, we had to find a way to estimate the density of states for the potential energy range contributing to the liquid-gas like phase transition which was sampled by a mixture of the two previously mentioned ensembles.

The gathered experiences with MC simulations in the NVE ensemble support the claim of Martin-Mayor⁴ of a practically non-existent exponential slowing down. Separate NVE MC simulations are sampling the potential energy region of the canonical phase transition. With the weighted histogram analysis method (WHAM) in the NVE ensemble, we are additionally able to transform the microcanonical sampling into canonical ensemble data.

This paper continues with a discussion of the microcanonical subensembles in Sec. II. Afterwards, we explain all the used simulation and analysis techniques in Sec. III. In Sec. IV, the gained knowledge is then applied to the collapse transition of a polymer, a 4-particle Lennard-Jones gas condensation, and the aggregation of a polymer system. The paper concludes in Sec. V with a summary of our main results.

II. MICROCANONICAL (SUB) ENSEMBLES

The constraints of linear momentum and angular momentum conservation in MD will restrict the NVE ensemble. Here, we define the total energy E as the sum of kinetic energy E_k and potential energy $E_p = U(\mathbf{x}_1, \dots, \mathbf{x}_N)$ where \mathbf{x}_i , $i = 1, \dots, N$ denote the particle positions. To be precise, angular momentum conservation in a MD simulation is only present when there is no influence from the periodic boundary conditions. For instance, the angular momentum is not conserved if the particles are further away from each other than half the box length. MD simulations with periodic boundary conditions may therefore encounter two different ensembles. If all simulated objects always keep a distance smaller than half the box length, as it is the case for a condensate or aggregate, the simulated ensemble is the NVEPJ ensemble (see Sec. II C). If the angular momentum is changing

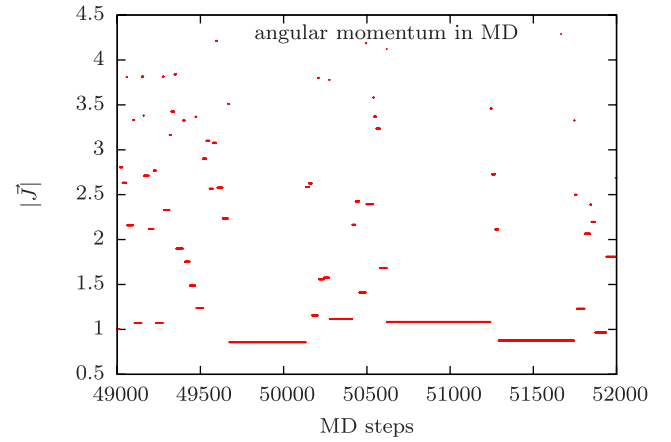


FIG. 1. Absolute values of the angular momentum during a MD simulation for a 4-particle Lennard-Jones system in a box of size 10^3 at a total energy per particle $e = -0.6$.

frequently, the MD simulation will sample the NVEP ensemble (see Sec. II B). At total energies in between those two regimes, the simulation will switch between states of fixed and fluctuating angular momentum (see Fig. 1).

A. NVE

The NVE ensemble contains all phase space points with a fixed total energy E at constant volume V and particle number N . It is possible to analytically integrate the momentum part of the phase space if the potential energy E_p is independent of the momenta (this will be the case for all the presented examples). This yields a configuration weight $W(E_p)$, defined by

$$\Gamma = \int_{\mathbf{X}} dx^{3N} W(E_p(\mathbf{x}_1, \dots, \mathbf{x}_N)). \quad (2)$$

Here, Γ stands for the partition function of the microcanonical ensemble. Expectation values are correspondingly given as

$$\langle O \rangle = \frac{\int_{\mathbf{X}} dx^{3N} O(\mathbf{x}_1, \dots, \mathbf{x}_N) W(E_p(\mathbf{x}_1, \dots, \mathbf{x}_N))}{\int_{\mathbf{X}} dx^{3N} W(E_p(\mathbf{x}_1, \dots, \mathbf{x}_N))}. \quad (3)$$

In the case of the NVE ensemble, we obtain¹²

$$\begin{aligned} \Gamma_{\text{NVE}} &= \int_{\mathbf{X}} \int_{\mathbf{P}} dx^{3N} dp^{3N} \delta(E - (E_k + E_p)) \\ &\propto \int_{\mathbf{X}} dx^{3N} (E - E_p)^{\frac{3N-2}{2}} \Theta(E - E_p), \end{aligned} \quad (4)$$

where Θ is the Heaviside step function. The configuration weight according to Eqs. (2) and (4) is in this case

$$W_{\text{NVE}}(E_p) = C(E - E_p)^{\frac{3N-2}{2}} \Theta(E - E_p), \quad (5)$$

with C as a constant normalization factor. To obtain a temperature expression for this ensemble, we choose the Boltzmann entropy definition

$$S(E) = k_B \ln \Gamma_{\text{NVE}}. \quad (6)$$

The temperature may then be derived from the relation

$$\frac{1}{T} = \beta = \left(\frac{\partial S}{\partial E} \right)_{N, V, (P, J)}. \quad (7)$$

For the NVE ensemble, we obtain

$$T(N, V, E) = \frac{2}{3N-2} \frac{1}{\langle \frac{1}{E_k} \rangle}. \quad (8)$$

For details on the derivation see also Pearson *et al.*²⁰ Equation (8) represents an alternative temperature definition to equipartition theorem Eq. (1) for the microcanonical ensemble. It can be derived directly from the partition function definition in Eq. (4) and was therefore chosen here in most cases except for comparisons. The prefactors in Eqs. (8) and (1) satisfy for the NVE ensemble ($f = 3N$) the relation $2/f = 2/3N < 2/(3N-2)$ while the inequality between the harmonic and arithmetic means leads to $\langle E_k \rangle \geq 1/\langle 1/E_k \rangle$.

Note that the entropy in microcanonical analyses of MC simulations is usually defined as $S(E_p) = k_B \ln \Omega(E_p)$, where $\Omega(E_p)$ is the density of states which quantifies the configuration volume with constant potential energy E_p . In Eq. (6), on the other hand, the entropy is defined as a function of the total energy $E = E_k + E_p$. One advantage of this fixed-total-energy (NVE) ensemble, which includes the kinetic energy, is the possibility to sample efficiently with a Metropolis-like scheme (see Sec. III A). For the fixed-potential-energy ensemble (NVE_p), it is, on the other hand, nontrivial to propose updates which still allow for a sufficient sampling of the available state space.

B. NVEP

If we consider the conservation of the total linear momentum $\mathbf{P} = \sum_{i=1}^N \mathbf{p}_i$, we end up with a different partition function,¹⁸

$$\begin{aligned} \Gamma_{\text{NVEP}} &= \int_{\mathbf{X}} \int_{\mathbf{P}} dx^{3N} dp^{3N} \delta(E - (E_k + E_p)) \delta\left(\mathbf{P} - \sum_{i=1}^N \mathbf{p}_i\right) \\ &\propto \int_{\mathbf{X}} dx^{3N} \left(E - E_p - \frac{\mathbf{P}^2}{2M}\right)^{\frac{3N-5}{2}} \Theta\left(E - E_p - \frac{\mathbf{P}^2}{2M}\right), \end{aligned} \quad (9)$$

where $M = \sum_{i=1}^N m_i$. Here, the configuration weight can be identified as

$$W_{\text{NVEP}}(E_p) = C \left(E - E_p - \frac{\mathbf{P}^2}{2M}\right)^{\frac{3N-5}{2}} \Theta\left(E - E_p - \frac{\mathbf{P}^2}{2M}\right), \quad (10)$$

with C as a normalization factor. For all cases considered in this study, we set $\mathbf{P} = 0$ for convenience.

C. NVEPJ

By introducing the conservation of the angular momentum $\mathbf{J} = \sum_{i=1}^N \mathbf{x}_i \times \mathbf{p}_i$, we get the partition function in the NVEPJ or molecular dynamics ensemble,¹²

$$\begin{aligned} \Gamma_{\text{NVEPJ}} &= \int_{\mathbf{X}} \int_{\mathbf{P}} dx^{3N} dp^{3N} \delta(E - (E_k + E_p)) \\ &\quad \times \delta\left(\mathbf{P} - \sum_{i=1}^N \mathbf{p}_i\right) \delta\left(\mathbf{J} - \sum_{i=1}^N \mathbf{x}_i \times \mathbf{p}_i\right) \end{aligned}$$

$$\begin{aligned} &\propto \int_{\mathbf{X}} dx^{3N} \frac{1}{\sqrt{\det(I)}} \left(E - E_p - \frac{\mathbf{P}^2}{2M} - \frac{1}{2} \mathbf{J}^T I^{-1} \mathbf{J}\right)^{\frac{3N-8}{2}} \\ &\quad \times \Theta\left(E - E_p - \frac{\mathbf{P}^2}{2M} - \frac{1}{2} \mathbf{J}^T I^{-1} \mathbf{J}\right), \end{aligned} \quad (11)$$

where we introduced the inertia tensor I ,

$$I_{jk} = \sum_{i=1}^N m_i [(x_{i1}^2 + x_{i2}^2 + x_{i3}^2) \delta_{jk} - x_{ij} x_{ik}], \quad (12)$$

with $j, k = 1, 2, 3$. The configuration weight is then expressed in the form

$$\begin{aligned} W_{\text{NVEPJ}}(E_p, I) &= C \frac{1}{\sqrt{\det(I)}} \left(E - E_p - \frac{\mathbf{P}^2}{2M} - \frac{1}{2} \mathbf{J}^T I^{-1} \mathbf{J}\right)^{\frac{3N-8}{2}} \\ &\quad \times \Theta\left(E - E_p - \frac{\mathbf{P}^2}{2M} - \frac{1}{2} \mathbf{J}^T I^{-1} \mathbf{J}\right), \end{aligned} \quad (13)$$

where C is again a normalization factor. It has to be mentioned that the NVEPJ configuration weight is more difficult to handle than that of the NVT, NVE, or NVEP ensemble. In the latter ensembles, the configuration weight can be reduced to a function of only the potential energy. The NVEPJ configuration weight, however, additionally includes the inertia tensor that also depends directly on the spatial coordinates.

III. SIMULATION METHODS

A. NVE Metropolis simulations

The microcanonical MC simulations were based upon configuration weights Eq. (5) presented in Sec. II A. In the same way as it is done for the canonical Metropolis MC acceptance probability, the microcanonical acceptance rate was chosen as the ratio of the configuration weights,

$$P_{\text{acc}}(A \rightarrow B) = \min\left(1, \frac{W_{\text{NVE}}(B)}{W_{\text{NVE}}(A)}\right). \quad (14)$$

Therefore, the acceptance probability for the NVE ensemble looks like

$$P_{\text{acc}}(A \rightarrow B) = \min\left(1, \left(\frac{E - E_p^B}{E - E_p^A}\right)^{\frac{3N-2}{2}} \frac{\Theta(E - E_p^B)}{\Theta(E - E_p^A)}\right). \quad (15)$$

The Θ -functions reflect the trivial fact that it is necessary to start simulations in a state where the potential energy E_p is smaller than the fixed total energy E . This simulation method was already presented, for example, in Refs. 11 and 21.

To investigate a phase transition, we started simulations at different total energies and measured the mean potential energy and temperature. This method allowed us a relatively easy sampling in the phase transition region which was already observed for a spin model.⁴

B. Multicanonical simulations

In order to generate independent benchmark results, we also performed Markov chain Monte Carlo simulations in the

multicanonical (MUCA) ensemble,^{22–25} which allows for an accurate estimation of expectation values in the canonical and microcanonical ensembles.^{24,25} The key idea of this method is to replace the Boltzmann weight in the canonical probability distribution by an *a priori* unknown weight function $W_{\text{MUCA}}(E_p)$ that is iteratively modified in order to yield a flat histogram in the potential energy space. In terms of the partition function, this reads

$$\begin{aligned} Z_{\text{MUCA}} &= \int_{\mathbf{x}} dx^{3N} W_{\text{MUCA}}(E_p(\mathbf{x}_1, \dots, \mathbf{x}_N)) \\ &= \int dE_p \Omega(E_p) W_{\text{MUCA}}(E_p), \end{aligned} \quad (16)$$

where $\Omega(E_p)$ is the density of states. This highlights that for a flat histogram, the weight function has to be essentially the inverse density of states $W_{\text{MUCA}}(E_p) \approx \Omega^{-1}(E_p)$. That way, the final data (production run with fixed weights) from a single simulation may be reweighted to any canonical and microcanonical distribution with time-series reweighting analogous to Sec. III D, if the according potential energy range is covered by the flat histogram.

The most demanding part is to obtain $W_{\text{MUCA}}(E_p)$. We applied both a naïve approach where successive weights are estimated from the histograms $H(E_p)$ of the previous iteration like $W_{\text{MUCA}}^{(n+1)}(E_p) = W_{\text{MUCA}}^{(n)}(E_p)/H(E_p)$, and a recursive version, where all previous histograms are incorporated in the estimation of successive weights.^{25,26} To this end, the potential energy space was discretized in the desired energy range, which in turn was obtained from a short parallel tempering simulation. In order to accelerate the iteration procedure and distribute the final production run to independent Markov chains, we applied a highly parallel implementation of the multicanonical method.²⁷

C. Molecular dynamics simulations with conserved total energy

In this work, we deliberately avoided the use of any thermostat. Therefore, the simulation only consisted of a numerical integration conserving the total energy up to a numerical error. The Velocity-Verlet integrator was used for the time integration. This simulation method might be appealing since it avoids the use of the frequently discussed thermostats.^{28,29} But we have to mention that our transformation into the NVT ensemble, which we will discuss later, will be without any dynamical information, while a thermostat aims for dynamical NVT data. The simulation runs in this work have been started several (10–20) times with different initial configurations. This has been done to address the problem of non-ergodicity when MD simulations are started from just one configuration.¹²

The total energy ranges for the NVEP and NVEPJ ensembles will be discussed in Sec. IV B. Apparently, it was necessary to calculate the angular momentum and the inertia tensor. We used the standard definition of the angular momentum,

$$\mathbf{J} = \sum_{i=1}^N \mathbf{x}_i \times \mathbf{p}_i, \quad (17)$$

where \mathbf{x}_i and \mathbf{p}_i are the spatial coordinate and momentum of particle i . We see that the angular momentum is not conserved if the vector \mathbf{x}_i is flipped in an instant while \mathbf{p}_i will remain continuous. This happens if due to the PBC, a particle changes position from one site of the box to another and it is one reason why the angular momentum is not conserved.

The use of the coordinates $\mathbf{x}_i = (x_i, y_i, z_i)$ requires a choice of the origin of the coordinate system. The origin was chosen as the center of mass (COM). This has been done to ensure that a condensate which is located at the border of the periodic boundary box still has a conserved angular momentum. Of course, this procedure is not measuring the correct angular momentum when the particles are in the gas phase. In this case, however, the angular momentum was no longer of interest. For details about the COM calculation, including the scheme of Bai and Breen,³⁰ see the Appendix.

D. Reweighting between different ensembles

Our aim was to compare the results of microcanonical MC to MD data. Therefore, we applied a reweighting technique from the NVEPJ/NVEP ensemble to the NVE ensemble. Since we know the configuration weights of the two ensembles, we can apply a time-series reweighting procedure if we have similar sampling ranges for the desired observable in both ensembles. The time-series reweighting from an NVEPJ ensemble into an NVE ensemble was applied in the following way:

$$\langle O \rangle_{\text{NVE}} = \frac{\left\langle O \frac{W_{\text{NVE}}(E_p)}{W_{\text{NVEPJ}}(E_p, T)} \right\rangle_{\text{NVEPJ}}}{\left\langle \frac{W_{\text{NVE}}(E_p)}{W_{\text{NVEPJ}}(E_p, T)} \right\rangle_{\text{NVEPJ}}}. \quad (18)$$

The configuration weights W_{NVE} and W_{NVEPJ} can be obtained from Eqs. (5) and (13). A similar formula can be formulated for the reweighting from the NVEP to the NVE ensemble.

The situation becomes a bit more complicated in cases where boundary conditions have to be considered. If the changes in angular momentum are frequent enough, the sampled histograms were in complete agreement with estimated NVEP histograms from reference MC simulations. However, so far, we found no proof that the PBC is switching the angular momentum in an appropriate way to guarantee sampling of the NVEP ensemble. Nonetheless, assuming NVEP sampling for frequent angular momentum shifts always led to consistent density of state estimates.

There are total energies with a low probability for angular momentum change. These cases were excluded from the analysis. We decided between the frequent and infrequent changes by setting a minimum number N_{min} of angular momentum changes N_a . If there was an angular momentum change in the simulation at all, the simulation was only considered for the analysis if $N_a > N_{\text{min}}$.

In this work, we determined N_{min} by comparing the obtained data from MD to the MC data. Normally, either MD or MC simulations are done and there would be no data for comparison. Alternatively, it would be possible to apply single-histogram reweighting to the simulated total energies. The total energy which has to be dismissed from the data set should then

be the one which is not predicted by the neighboring results from nearby total energies.

E. WHAM procedure for microcanonical sampling data

The density of states $\Omega(E_p)$ is a useful quantity. It provides a way to reduce the partition function from a configuration integral to a potential energy integral,

$$\begin{aligned}\Gamma_{\text{NVE}} &= \int_{\mathbf{x}} dx^{3N} W_{\text{NVE}}(E_p(\mathbf{x}_1, \dots, \mathbf{x}_N)) \\ &= \int_E dE_p \Omega(E_p) W_{\text{NVE}}(E_p),\end{aligned}\quad (19)$$

where $W_{\text{NVE}}(E_p)$ is the microcanonical configuration weight in Eq. (5). WHAM^{31,32} can be used to get an estimate for the density of states of a system from multiple canonical potential energy histograms, for example, from a parallel tempering simulation. The density of states is a universal property of the system which can be used to calculate averages in different ensembles if the appropriate weight function of the ensemble $W(E_p)$ is known. In Ref. 33, a WHAM formula is given for a general configuration weight and we inserted $W_{\text{NVE}}(E_p)$ to obtain the following NVE-WHAM formulas. This way, we got an estimate for the density of states from M microcanonical MD simulations at different total energies $E^{(m)}$, $m = 1, \dots, M$. A similar approach with a different multi-histogram technique can be found in Refs. 10 and 12. The first step was to reweight the MD simulation results to a histogram in the NVE ensemble. We measured histograms with a chosen resolution by interpreting the bin of a potential energy histogram as an observable,

$$H(E_i) = \langle \delta(E_p, E_i) \rangle, \quad (20)$$

where i is the bin index. An approximation for an NVE histogram was obtained by the use of time-series reweighting for each histogram bin.

The main part of the WHAM procedure is the recursive calculation of the normalization constants Γ_m from the obtained NVE histograms

$$W_{\text{NVE}^{(m)}}(E_p) = (E^{(m)} - E_p)^{\frac{3N-2}{2}} \Theta(E^{(m)} - E_p), \quad (21)$$

$$\Omega(E_p, \Gamma_1, \dots, \Gamma_M) = C \frac{\sum_{m=1}^M H_m(E_p)}{\sum_{m=1}^M N_m \frac{1}{\Gamma_m} W_{\text{NVE}^{(m)}}(E_p)}, \quad (22)$$

$$\Gamma_m = \sum_{E_p=E_{\min}}^{E^{(m)}} \Omega(E_p, \Gamma_1, \dots, \Gamma_M) W_{\text{NVE}^{(m)}}(E_p), \quad (23)$$

where the sum over $m = 1, \dots, M$ is the sum over the histograms for different total energies $E^{(m)}$, N_m is the number of measurements for the estimation of the m th histogram, E_{\min} is the sampled minimum potential energy of all M histograms, and C is a constant prefactor. Note that in Eq. (23), $E^{(m)}$ is the upper bound of the sum since $\Theta(E^{(m)} - E_p)$ sets the summation arguments for the remaining potential energies to zero. The histograms were ordered according to their total energies in a manner that the total energy $E^{(m)}$ increases with m . In the iteration procedure, we choose $\Gamma_1 = 1$ by setting the prefactor C .

The estimated density of states was afterwards used for the computation of ensemble averages. For observables which depend only upon the potential energy, we calculated the observable average at various total energies in the NVE ensemble,

$$\langle O \rangle_{\text{NVE}} = \frac{\sum_{E_p=E_{\min}}^E O(E_p) \Omega(E_p) (E - E_p)^{\frac{3N-2}{2}}}{\sum_{E_p=E_{\min}}^E \Omega(E_p) (E - E_p)^{\frac{3N-2}{2}}} \quad (24)$$

and various temperatures in the NVT ensemble,

$$\langle O \rangle_{\text{NVT}} = \frac{\sum_{E_p=E_{\min}}^{E_{\max}} O(E_p) \Omega(E_p) e^{-\frac{E_p}{T}}}{\sum_{E_p=E_{\min}}^{E_{\max}} \Omega(E_p) e^{-\frac{E_p}{T}}}, \quad (25)$$

where E_{\max} is the maximum potential energy of all M histograms. That way, we obtain caloric curves in the NVE and NVT ensembles.

The iteration-free ST-WHAM procedure³³ is an interesting alternative for the estimation of the density of states.³⁴⁻³⁷ It directly yields $\beta_{\text{NVE}_p} = \partial \ln \Omega(E_p) / \partial E_p$ in the NVE_p ensemble, which is shown in Fig. 2 (top) for the example of polymer aggregation (discussed in detail in Sec. IV C). The result is in good agreement with estimates from NVE-WHAM and MUCA simulations, numerically differentiating $\ln \Omega(E_p)$

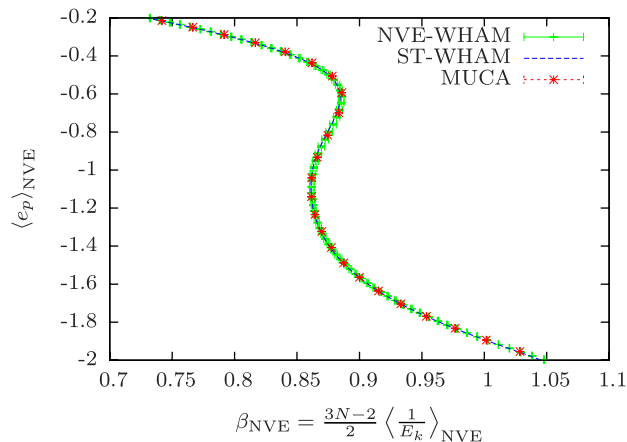
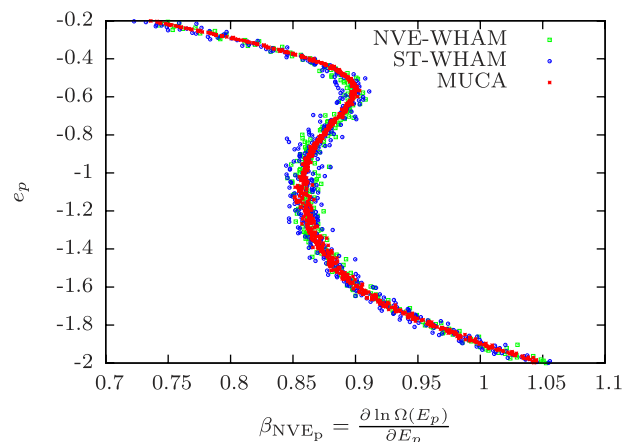


FIG. 2. Comparison of ST-WHAM results to NVE-WHAM and MUCA for the example of polymer aggregation (see Sec. IV C). Microcanonical potential energy vs. inverse temperature plot for the NVE_p (top) and NVE ensembles (bottom).

with a five-point derivative. Recall that, as mentioned at the end of Sec. II A, the NVE and NVE_p ensembles are not equivalent for finite systems. Hence, the inverse temperatures β_{NVE} and β_{NVE_p} , as well as the resulting caloric curves differ especially in the phase-transition region. Starting with the ST-WHAM procedure, the desired caloric NVE curves may be obtained by first integrating β_{NVE_p} which yields $\Omega(E_p)$. Then, Eq. (24) gives, within error range, compatible caloric NVE curves shown in Fig. 2 (bottom).

F. Summary of the MD simulations and their analysis

In case an interested reader wants to reproduce the obtained results, we like to summarize the MD simulation and data analysis methods.

1. MD simulation

Start energy conserving MD simulations for various total energies.

- Measure angular momentum, inertia tensor, potential energy, and temperature.
- Repeat the simulations for different start configurations.

2. Reweighting procedure

Reweighting between different ensembles. For each total energy, we perform the following steps.

- Measure the number of angular momentum changes N_a . If $N_a = 0$, use the NVEPJ ensemble, if $N_a > N_{\text{min}}$, use the NVEPJ ensemble, and discard the total energy if $0 < N_a \leq N_{\text{min}}$.
- Reweight the observable from the simulated to the NVE ensemble.
- Apply the jackknife procedure to estimate error bars.³⁸

3. NVE-WHAM

Apply the NVE-WHAM procedure to various simulations at constant total energy with a potential energy overlap.

- Use the reweighting procedure for the histogram bins to get histograms in the NVE ensemble.
- Estimate the density of states by iterative calculation of Γ_m in Eqs. (22) and (23).
- Use the estimated density of states for the calculation of the average potential energy and temperature at various total energies in the NVE ensemble [Eq. (24)]. Additionally, calculate the average potential energy in the NVT ensemble at various temperatures [Eq. (25)].
- Apply the procedure again to several subsets of the data set to estimate an error bar.

IV. APPLICATIONS

A. Polymer collapse

As the most simple test case, we consider the collapse of a single polymer. For a single polymer, the simulation box

can be always chosen large enough that boundary conditions do not matter. The center of mass and angular momentum will be conserved in MD. In this case, the MD simulation will run completely in the NVEPJ ensemble. The polymer had a length of $N = 13$ monomers such that $f = 3N - 6 = 33$ and we simulated total energies per monomer $e (= E/N)$ from $e = -2$ to $e = 2$ in $\Delta e = 0.2$ intervals. The mass of each particle was set to $m_i = 1$. For the interactions of the monomers, we took a Lennard-Jones (LJ) potential

$$U_{\text{LJ}}(r) = 4\epsilon \left(\left(\frac{\sigma}{r} \right)^{12} - \left(\frac{\sigma}{r} \right)^6 \right) \quad (26)$$

with parameters $\epsilon = 1$, $\sigma = 0.7/\sqrt[6]{2}$, and a cutoff at $r_c = 2.5\sigma$ together with a potential shift of $-U_{\text{LJ}}(r_c)$. The bond interactions were modeled by the FENE (finitely extensible nonlinear elastic) potential

$$U_{\text{FENE}}(r) = -\frac{K}{2}R^2 \ln \left(1 - \left[\frac{(r-r_0)}{R} \right]^2 \right) \quad (27)$$

with the parameters $K = 40$, $R = 0.3$, and $r_0 = 0.7$. Those interaction parameters are the same as in Refs. 39 and 40. The FENE potential has a steep increase if r approaches $r_0 \pm R$ and the time step has to be relatively small to do the time integration for this potential. The chosen time step was $\Delta t = 0.0001$. This was still not sufficient to keep the integrator from occasionally yielding bonded-monomer distances $|r - r_0| > R$ (resulting in divergences of the logarithm). Therefore, we introduced restore points and simulated integration ranges again with smaller time steps if the simulation had encountered divergences. Hence, we could avoid to use extremely small time steps for the whole simulation. Measurements were done every 600 integration steps. A total number of 10^5 measurements were performed. For this test case, it was easy to illustrate the differences between an NVE MC simulation and an NVEPJ MD simulation.

Figure 3 (top) shows a comparison between the different simulation techniques. Each point is the result of a simulation at a fixed total energy and, in case of the MD simulations, at zero angular and linear momentum. The kinetic energy and the potential energy are the observables. The mean values for those observables are shown with their respective errors. The jackknife procedure was applied to the data to estimate the error bar.

At first we like to highlight that the MUCA data are in all cases within the error range of the NVE Metropolis data. We therefore consider both simulation techniques to be in agreement. We see, on the other hand, a difference between the NVE Metropolis simulation and the MD simulation in the NVEPJ ensemble (in the plot “MD direct”). Systematic deviations were obtained between the averages from MD and NVE Metropolis which are exceeding the error ranges. Those deviations disappear when the MD data are reweighted to the NVE ensemble (“MD reweighted”). Hence, we see that the MD and MC simulations are sampling in different ensembles (NVEPJ and NVE, respectively).

Even for this small number of degrees of freedom, the differences are much smaller if we apply the respective temperature definitions. Equipartition theorem Eq. (1), which

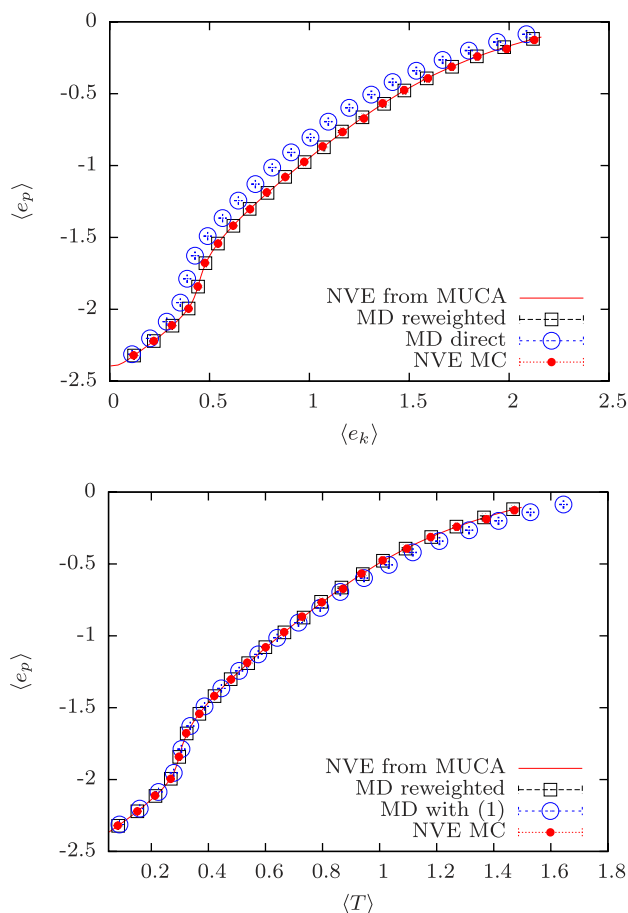


FIG. 3. Microcanonical behavior of the $N = 13$ bead spring polymer. (top) Potential vs. kinetic energy plot for the collapse transition. (bottom) Potential energy vs. microcanonical temperature diagram. In both cases, the error bars are smaller than the size of the data symbols.

is the standard definition for most of the MD packages, was applied to the raw MD data and corrects to some extent the differences between the ensembles (see Fig. 3 (bottom)). This curve therefore represents the expected results from a standard MD package. For the calculation of the temperature of the reweighted MD data and all the MC data, we used Eq. (8). The unweighted data points, analysed with Eq. (1), are closer to the NVE data for the same total energy but the deviation is still larger than 3 times the error range. An interesting behavior is that the equipartition theorem shifts the MD points onto the NVE data from MUCA but only within the error range of points which are corresponding to higher total energies. So while the points which were evaluated with Eq. (1) are not within the error range of the NVE data for the same total energy from the MC simulations, they are within the error range of NVE data for higher total energies. This statement holds apparently in a temperature range from 0.1 to around 0.8. Therefore, one would obtain with Eq. (1) the same curve where all single points are shifted. This behavior becomes important for the density of states estimation for the following examples.

As we see in Fig. 3 (bottom), the reweighting procedure for the MD data in the NVEPJ ensemble to observable averages in the NVE ensemble was quite successful. The obtained reweighted MD data are within the error range of the MC simulations.

B. Lennard-Jones gas condensation

A simple 4-particle LJ system with periodic boundary conditions was considered to investigate the behavior of the two involved ensembles in MD. The three-dimensional simulation box had a linear length of $L = 10$. The LJ parameters were the same as for the monomers of the single polymer example, but here without a cutoff. The mass of each particle was again $m_i = 1$. The time step was $\Delta t = 0.001$. Measurements were done every 400 steps.

All the total energies e for which we did simulations are shown in Fig. 4 together with the number of angular momentum changes in the respective simulations. There are two different ensemble regimes for the MD simulations depending on the total energy. At low total energies, and therefore for the LJ condensate, we encountered an NVEPJ ensemble exactly like we observed it for the single polymer. At a total energy per particle of $e = -0.7$, a single particle occasionally separates from the condensate but with a rather low number of angular momentum changes, $N_a = 313$ after 1×10^6 measurements. The minimum number of angular momentum switches was set to $N_{\min} = 1000$ for this system. Therefore, the total energy $e = -0.7$ was dismissed from the data. At the slightly higher total energy of $e = -0.65$, the number of angular momentum changes was already up to $N_a = 5608$ and the simulation could be considered to be in the NVEP ensemble. The transition from the NVEPJ to the NVEP ensemble can be seen as well in the corresponding histograms in Fig. 5. The figure shows the results of an application of the reweighting technique under the assumption of different ensembles at different total energies. The assumption of an NVEPJ ensemble reproduces the data from comparative MUCA simulations quite accurately for a total energy of $e = -0.75$. For a total energy of $e = -0.65$, the NVEP ensemble assumption is the one that is able to reproduce the MUCA histogram (see Fig. 5), including the secondary peak at $e_p \approx -0.74$ which reflects the already mentioned separation of one particle from the condensate.

The WHAM procedure was applied to the reweighted NVE histograms. The obtained density of states has been used to calculate the average temperature and potential energies for various total energies in the NVE ensemble according

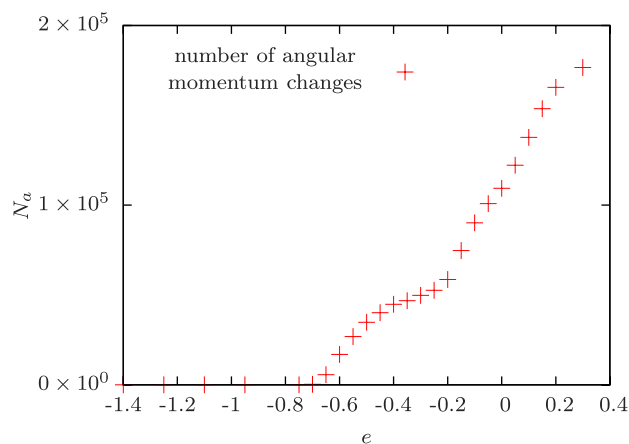


FIG. 4. Number of angular momentum changes for the simulated total energies of the 4-particle LJ system.

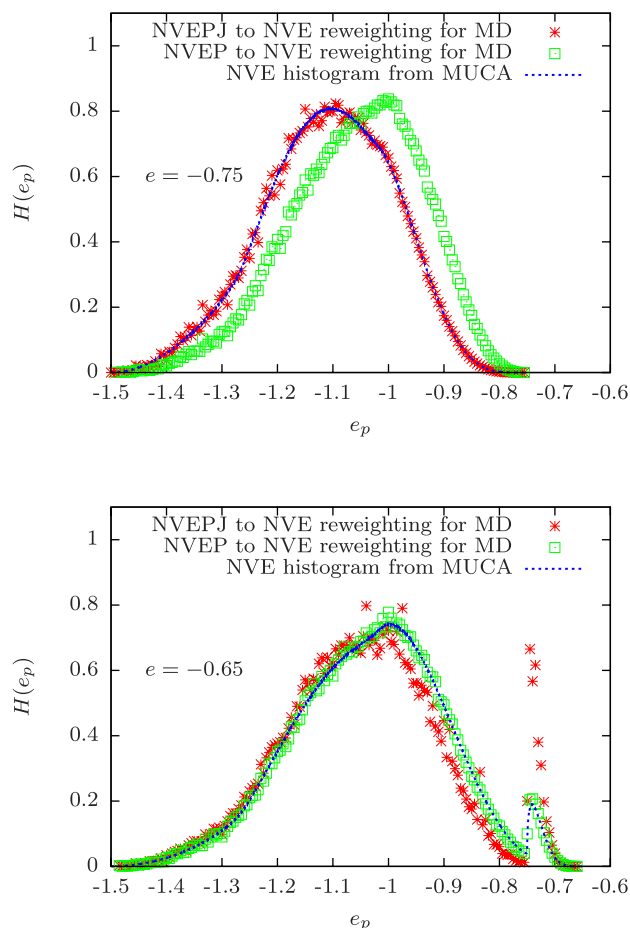


FIG. 5. Resulting histograms for the 4-particle LJ system after the application of reweighting procedures from NVEPJ to NVE and NVEP to NVE. The top and bottom histograms are at a total energy of $e = -0.75$ and $e = -0.65$, respectively.

to Eq. (24) and various temperatures in the NVT ensemble according to Eq. (25). The results are shown in Fig. 6 (top) with statistical errors according to Sec. III F. It shows that it was possible to obtain the same result as we got it from MUCA simulations if we regard the error ranges. The “MD reweighted” points each represent the reweighted result from a single simulation at fixed total energy.

The NVE curve shows three local maxima of temperature for different potential energies. This is the so-called “back bending effect.”¹ Those three energies mark successive separations of LJ particles from the cluster which happen with an increasing probability in a total energy range around those maxima. The lowest potential energy corresponds to the onset of angular momentum changes at $e = -0.7$ noted previously in the discussion of Fig. 4. Similar observations have been made for quite different systems.^{14,41}

Notable is that, after the WHAM procedure is performed successfully, it is possible to obtain the NVT data from a lot of MD simulations without the use of a thermostat. However, since every dynamical information is lost, we lose one of the main advantages of MD.

The 4-particle LJ system has even less degrees of freedom ($f_{\text{NVEPJ}} = 6$ and $f_{\text{NVEP}} = 9$) than the single polymer. Therefore, it is not surprising that the temperature definition according to the equipartition theorem induces even bigger deviations than

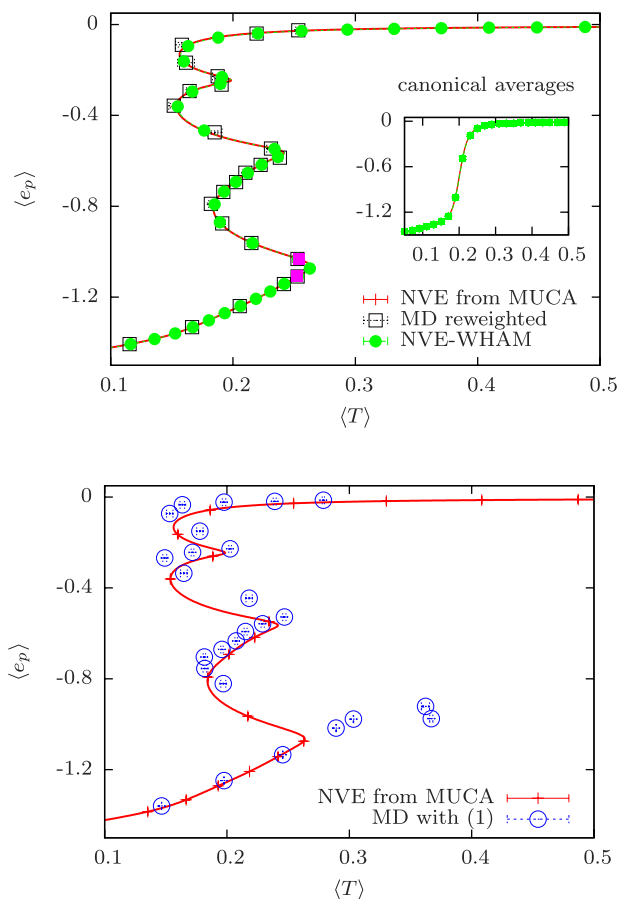


FIG. 6. Microcanonical potential energy vs. temperature plot for the 4-particle LJ system nucleation. (top) Comparison of several methods using the full reweighting procedure. The filled purple squares are averages for the total energies $e = -0.65$ and $e = -0.75$. The inset shows the corresponding result in the canonical ensemble. (bottom) The MD data is evaluated with Eq. (1) by inserting the appropriate number of degrees of freedom.

we observed for the single polymer (see Fig. 6 (bottom)). The points which are furthest from the MUCA data could be explained by the difficulty to assign a number for the degrees of freedom to the total energy region around $e = -0.7$ with infrequent angular momentum shifts.

C. Polymer aggregation

As an example that is closer to everyday life in computational physics, we choose a system of 8 polymers with 13 monomers each. The system was placed in a periodic box of length $L = 30$. The interaction parameters and monomer masses are the same as in Sec. IV A and the intermolecular interaction among the 8 polymers was chosen to be identical to the intramolecular interaction. The time step was $\Delta t = 0.0001$ and the restore point procedure was again applied to deal with the FENE potential. Measurements were taken every 2400 steps and 2×10^6 measurements were collected for each total energy. In this case, it was harder to ensure ergodicity and 20 MD runs were performed for each total energy. We simulated energies from $e = -0.6$ to $e = 1.4$ in intervals of $\Delta e = 0.2$. We dismissed the total energy of $e = -0.4$ from the simulation data because the averages were not consistent with the expected ones from MC simulations. At this energy, the

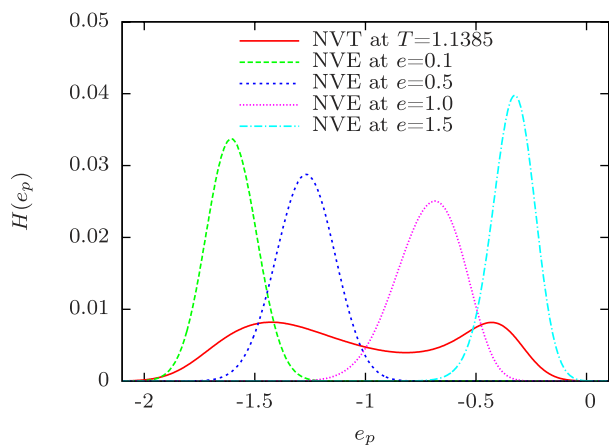


FIG. 7. NVE and NVT histograms in the phase-transition region for the 8×13 polymer system.

number of angular momentum shifts was $N_a = 4411$ which is too infrequent to assume an NVEP ensemble behavior for this system. We set the minimum number of angular momentum shifts in the analysis program to $N_{\min} = 10000$. Only at the lowest considered total energy $e = -0.6$, no angular momentum changes occurred and an NVEPJ ensemble behavior was observed.

The NVE Metropolis simulation used single-bead translation and polymer translation as update moves. It required less computation time for all points (computed in parallel) than the complete parallel MUCA simulation. Of course, we obtain more detailed data from MUCA with smaller error bars but it is still noticeable that the microcanonical MC simulation samples the potential energy interval of the canonical first-order phase transition without any problems. This effect might be explained by the microcanonical sampling. The energy range which was relevant for the phase transition was covered by several single-peak histograms from NVE simulations at several total energies (see Fig. 7). The canonical histogram showed a double peak which was not present in the different NVE runs. Therefore, it was necessary to start several NVE simulations to cover the relevant potential energy range but one does not expect, and we did not observe exponential slowing down for the single runs. This behavior of the microcanonical ensemble has been described in Ref. 4 for the Potts model.

The MC simulation, the reweighted MD data, and the MUCA data are within 3 times the error range (see exemplary Table I and Fig. 8 (top)). The MD data which were evaluated with the equipartition theorem ($f_{\text{NVEPJ}} = 306$ and $f_{\text{NVEP}} = 309$) are within 3–4 times the error range of the MC data (Fig. 8 (bottom)). For the data points which are evaluated with the temperature definition Eq. (1), we observed the same effect as in the application example IV A. Those averages,

TABLE I. Measured potential energies at total energy $e = 0$.

Method	Potential energy e_p
MD not reweighted	-1.6233(30)
MD reweighted	-1.6346(40)
MC	-1.6368(5)
MUCA	-1.6357(3)

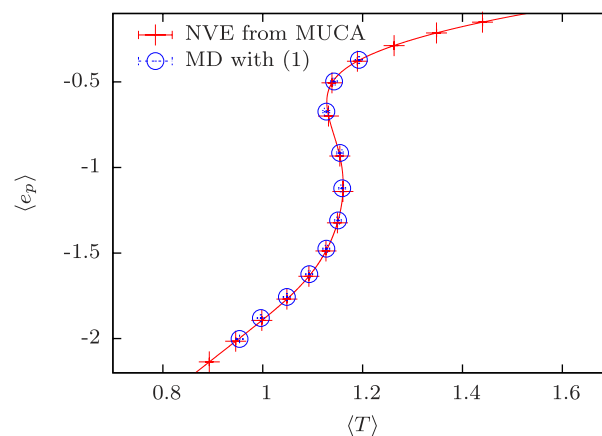
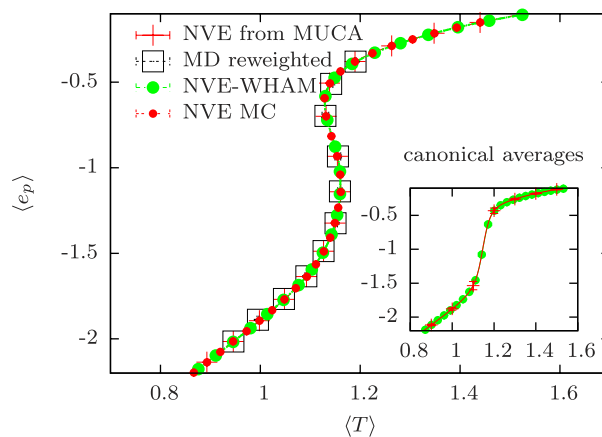


FIG. 8. Microcanonical potential energy vs. temperature plot for 8×13 polymer aggregation in a periodic box of length $L = 30$. (top) Comparison of several methods using the full reweighting procedure. The inset shows the corresponding result in the canonical ensemble. (bottom) The MD data is evaluated with Eq. (1) by inserting the appropriate number of degrees of freedom.

which were simulated for one total energy, are within the error range of averages we got from MUCA for slightly higher total energies. That means that the analysis with Eq. (1) would most likely result in the same curve where the single points are just slightly shifted. Therefore, the differentiation between the concrete ensembles is only necessary for the density of states estimation where it is crucial that the histogram corresponds to the simulated total energy.

V. CONCLUSIONS

We have carried out a detailed analysis of the ensemble behavior of MD simulations for the collapse transition and liquid-gas like transition for three exemplary systems. With a careful consideration of the conservation laws, we could match the dynamical MD and stochastic MC data for those phase transitions. For the presented systems with a small number of degrees of freedom (single polymer, Lennard-Jones system), the differences between the NVEPJ, NVEP, and NVE ensembles are prominent. The knowledge of the sampled ensembles and the similar sampling ranges allowed us to apply time-series reweighting into the NVE ensemble. The so obtained averages from MD simulations are within the error range of the MC data. We found that the liquid-gas like

transition, simulated by MD, undergoes an ensemble switch from the NVEPJ to the NVEP ensemble due to the periodic boundary conditions.

For the studied many polymer system, it was obvious that the commonly used equipartition theorem takes account of the constraints in the NVEP and NVEPJ ensembles in a good manner. The appropriate numbers of degrees of freedom have to be inserted for the aggregated and fragmented phase, respectively. The so achieved averages are within about three times the error range of the MC simulation data. With the effort of a time-series reweighting it was possible to eliminate the remaining systematic deviations caused by the temperature definition in Eq. (1). For a large number of degrees of freedom, these corrections are only relevant for theoretical considerations and strict quantitative comparison. In application of MD to realistic systems, the uncertainty of the model parameters would, most probably, cause greater deviations than the one we observed in comparison with the MC data.

A potential limitation of the presented procedure is the problem to produce ergodic data from MD simulations. The application examples are suggesting that it was possible to get ergodic data from MD by performing simulations from various initial conditions. There are techniques in the literature which propose other ways to get ergodic MD data.¹² The idea is to initialize the MD simulations with configurations which are obtained from MC simulations in the appropriate ensemble. Those techniques are promising for a combination with the proposed reweighting scheme and the NVE-WHAM procedure.

The NVE-WHAM procedure is relatively sensitive to deviations in the histogram. Therefore, this method benefits from a careful consideration of the conservation laws to estimate the density of states. According to our results for the density of states estimation it is really necessary to reweight to the NVE ensemble before applying the multi-histogram method. This is done by using the appropriate configuration weight of the NVEP or NVEPJ ensemble.

The surprisingly efficient sampling of the phase transitions in the NVE ensemble supports the work of Martin-Mayor for the Potts model.⁴ For the investigated phase transitions, no strongly suppressed energy regions were observed in the histograms, and therefore, no pronounced slowing down for the individual runs at separate total energies (see Fig. 7).

To conclude, when combined with the proposed NVE-WHAM procedure, simulations in the NVE ensemble offer the possibility to investigate phase transitions in the microcanonical ensemble in an efficient way and transform the gathered data afterwards into the canonical ensemble.

ACKNOWLEDGMENTS

This project was funded by the European Union and the Free State of Saxony, the ESF Junior Research Group No. 241 202, the Leipzig Graduate School GSC185 “BuildMoNa,” the DFG under Grant No. JA 483/24-3, and the Graduate College of the Deutsch-Französische Hochschule (DFH-UFA) under Grant No. CDFA-02-07. For the provided computing

time, we thank the John von Neumann Institute for Computing (NIC) who gave us access to the supercomputer JUROPA at Jülich Supercomputing Centre (JSC) under Grant No. HLZ21.

APPENDIX: CENTER OF MASS CALCULATION

The center of mass in PBC is evaluated in two steps. First, an estimate of the COM was calculated with the scheme from Bai and Breen which allows a straightforward handling of the PBC.³⁰ Afterwards, this estimate was used as the origin of the coordinate system to apply the usual COM definition. The COM was calculated for each coordinate separately. Consider, for example, the x coordinates of the system. Each particle's $x_i \in [-L/2, L/2)$ was mapped on the boundary of a unit circle in the $\xi - \psi$ plane,

$$\varphi_i = \frac{2\pi}{L}x_i, \quad \xi_i = \cos(\varphi_i), \quad \psi_i = \sin(\varphi_i). \quad (\text{A1})$$

Then, the averages of these coordinates are

$$\bar{\xi} = \frac{1}{N} \sum_{i=1}^N \xi_i, \quad \bar{\psi} = \frac{1}{N} \sum_{i=1}^N \psi_i. \quad (\text{A2})$$

The corresponding polar angle ϕ in the range $[-\pi, \pi)$ was obtained as

$$\phi = \text{ang}(\bar{\xi}, \bar{\psi}), \quad (\text{A3})$$

$$\text{ang}(\xi, \psi) = \begin{cases} \arccos\left(\frac{\xi}{\sqrt{\xi^2 + \psi^2}}\right), & \psi \geq 0, \\ -\arccos\left(\frac{\xi}{\sqrt{\xi^2 + \psi^2}}\right), & \psi < 0, \end{cases} \quad (\text{A4})$$

which yields the retransformed COM estimate in the range $[-L/2, L/2)$,

$$\tilde{x}_{\text{COM}} = \frac{L}{2\pi} \phi. \quad (\text{A5})$$

By applying this procedure to each coordinate, we got the first estimate for the center of mass $\tilde{\mathbf{x}}_{\text{COM}} = (\tilde{x}_{\text{COM}}, \tilde{y}_{\text{COM}}, \tilde{z}_{\text{COM}})$.

In the second step, this was used as the origin of the coordinate system to calculate the COM according to the usual definition (for particles with equal masses),

$$\mathbf{x}_{\text{COM}} = \frac{1}{N} \sum_{i=1}^N \mathbf{x}'_i, \quad (\text{A6})$$

where $\mathbf{x}'_i = \mathbf{x}_i - \tilde{\mathbf{x}}_{\text{COM}}$ is the relative coordinate with regard of the minimum-image convention in PBC. We followed up with this definition of the center of mass because it is the quantity that is conserved by Newton's equations of motion. Therefore, it will remain constant up to a numerical error. This center of mass was then finally used as the origin of the coordinate system for the calculation of the angular momentum and the inertia tensor.

¹D. H. E. Gross, *Microcanonical Thermodynamics: Phase Transitions in “Small” Systems* (World Scientific, Singapore, 2001).

²W. Janke, *Nucl. Phys. B* **63**, 631 (1998).

³C. Junghans, M. Bachmann, and W. Janke, *Phys. Rev. Lett.* **97**, 218103 (2006).

- ⁴V. Martin-Mayor, *Phys. Rev. Lett.* **98**, 137207 (2007).
- ⁵T. Chen, L. Wang, X. Lin, Y. Liu, and H. Liang, *J. Chem. Phys.* **130**, 244905 (2009).
- ⁶A. Hüller, *Z. Phys. B* **93**, 401 (1994).
- ⁷I. R. McDonald and K. Singer, *J. Chem. Phys.* **52**, 2166 (1970).
- ⁸J. Barker, R. Fisher, and R. Watts, *Mol. Phys.* **21**, 657 (1971).
- ⁹J. D. Honeycutt and H. C. Andersen, *J. Phys. Chem.* **91**, 4950 (1987).
- ¹⁰F. Calvo and P. Labastie, *Chem. Phys. Lett.* **247**, 395 (1995).
- ¹¹R. Lustig, *J. Chem. Phys.* **109**, 8816 (1998).
- ¹²F. Calvo, J. P. Neirrotti, D. L. Freeman, and J. D. Doll, *J. Chem. Phys.* **112**, 10350 (2000).
- ¹³J. Schluttig, M. Bachmann, and W. Janke, *J. Comput. Chem.* **29**, 2603 (2008).
- ¹⁴L. Gai, T. Vogel, K. A. Maerzke, C. R. Iacovella, D. P. Landau, P. T. Cummings, and C. McCabe, *J. Chem. Phys.* **139**, 054505 (2013).
- ¹⁵C. Junghans, D. Perez, and T. Vogel, *J. Chem. Theory Comput.* **10**, 1843 (2014).
- ¹⁶D. T. Seaton, S. Schnabel, D. P. Landau, and M. Bachmann, *Phys. Rev. Lett.* **110**, 028103 (2013).
- ¹⁷M. Marenz, J. Zierenberg, H. Arkin, and W. Janke, *Condens. Matter Phys.* **15**, 43008 (2012); M. Marenz and W. Janke, *Phys. Proc.* **57**, 53 (2014).
- ¹⁸R. Lustig, *J. Chem. Phys.* **100**, 3048 (1994).
- ¹⁹J. L. Lebowitz, J. K. Percus, and L. Verlet, *Phys. Rev.* **153**, 250 (1967).
- ²⁰E. M. Pearson, T. Halicioglu, and W. A. Tiller, *Phys. Rev. A* **32**, 3030 (1985).
- ²¹J. R. Ray, *Phys. Rev. A* **44**, 4061 (1991).
- ²²B. A. Berg and T. Neuhaus, *Phys. Lett. B* **267**, 249 (1991).
- ²³B. A. Berg and T. Neuhaus, *Phys. Rev. Lett.* **68**, 9 (1992).
- ²⁴W. Janke, *Int. J. Mod. Phys. C* **03**, 1137 (1992).
- ²⁵W. Janke, *Physica A* **254**, 164 (1998).
- ²⁶W. Janke, "Histograms and all that," in *Computer Simulations of Surfaces and Interfaces*, NATO Science Series, II. Mathematics, Physics and Chemistry, edited by B. Dünweg, D. P. Landau, and A. I. Milchev (Kluwer, Dordrecht, 2003), Vol. 114, pp. 137–157.
- ²⁷J. Zierenberg, M. Marenz, and W. Janke, *Comput. Phys. Commun.* **184**, 1155 (2013).
- ²⁸T. Soddemann, B. Dünweg, and K. Kremer, *Phys. Rev. E* **68**, 046702 (2003).
- ²⁹E. A. Koopman and C. P. Lowe, *J. Chem. Phys.* **124**, 204103 (2006).
- ³⁰L. Bai and D. Breen, *J. Graphics, GPU, Game Tools* **13**, 53 (2008).
- ³¹A. M. Ferrenberg and R. H. Swendsen, *Phys. Rev. Lett.* **63**, 1195 (1989).
- ³²S. Kumar, J. M. Rosenberg, D. Bouzida, R. H. Swendsen, and P. A. Kollman, *J. Comput. Chem.* **13**, 1011 (1992).
- ³³J. Kim, T. Keyes, and J. E. Straub, *J. Chem. Phys.* **135**, 061103 (2011).
- ³⁴L. G. Rizzi and N. A. Alves, *J. Chem. Phys.* **135**, 141101 (2011).
- ³⁵M. Church, C. Ferry, and A. E. van Giessen, *J. Chem. Phys.* **136**, 245102 (2012).
- ³⁶J. Kim, J. E. Straub, and T. Keyes, *J. Phys. Chem. B* **116**, 8646 (2012).
- ³⁷N. A. Alves, L. D. Morero, and L. G. Rizzi, *Comput. Phys. Commun.* **191**, 125 (2015).
- ³⁸B. Efron, *The Jackknife, the Bootstrap and Other Resampling Plans* (Society for Industrial and Applied Mathematics, Philadelphia, 1982).
- ³⁹J. Zierenberg, M. Mueller, P. Schierz, M. Marenz, and W. Janke, *J. Chem. Phys.* **141**, 114908 (2014).
- ⁴⁰J. Zierenberg and W. Janke, *Europhys. Lett.* **109**, 28002 (2015).
- ⁴¹C. Junghans, M. Bachmann, and W. Janke, *Europhys. Lett.* **87**, 40002 (2009).